Quantitative Evaluation of Near-Fault Records Generated via Wavelet Transform

Amin Gholizad[1] and Arash Pursadrollah[2*]

1. Associate Professor, Engineering Department, University of Mohaghegh Ardabili Ardabil, Iran, *Corresponding Author; email: gholizad@uma.ac.ir
2. M.Sc. Student, Engineering Department, University of Mohaghegh Ardabili, Ardabil

Received: 16/03/2015
Accepted: 03/01/2017

ABSTRACT

Nonlinear time-history analysis is becoming more common in seismic analysis and design of structures. The key issue in performing this kind of analysis is the appropriate input ground motion. Many engineers select recorded motions from locations other than the project site and modify them by scaling or spectrum matching. A wavelet-based procedure has been used to generate ground motions that are design spectrum compatible. Near-fault ground motions containing strong velocity pulses are of interest in the fields of seismology and earthquake engineering. Sites located in the vicinity of seismic faults may experience ground motions with the effect of forward directivity, causing most of the seismic energy in a single pulse registered early in the velocity history. Baker introduced a quantitative way to distinguish and classify this kind of records. The principle purpose of this article is to survey generating spectrum-compatible time-histories for near-fault via wavelet transform by Baker's method.

Keywords:
Wavelet transform; Artificial ground motion; Near-fault earthquakes; Spectrum-matching

1. Introduction

For seismic design of critical structures such as power plants, dams, tall buildings, and cable-stayed bridges in seismically active regions, the final design is usually based on a complete time-history analysis. It is difficult and nearly impossible in some cases to choose a proper record for design area when the recorded and processed accelerograms of the design location are few. Many engineers select recorded motions from locations other than the project site and modify them by scaling or spectrum matching.

The response of structures under earthquake ground motions can be calculated either using a response spectrum or an acceleration time history. For design purposes, the seismic codes provide a design spectrum, i.e. a smooth response spectrum that (hopefully) takes into account every possible earthquake likely to occur in a given zone (with a certain probability of occurrence). Because special care is taken to define a reliable design spectrum, and since the response spectrum method is a simple and well-established procedure, it is the most common approach to perform linear analysis of buildings and other conventional structures. However, the seismic analysis of many critical structures as mentioned before is usually done using a step-by-step time analysis. The major deficiency of the response spectrum analysis is its inability to provide temporal information of the structural responses. Such information is sometimes essential in attaining the satisfactory design. On the other hand, the ground motion time histories supply a full description of the earthquake motion, but the response spectrum exhibit duration

as well as amplitude and frequency content.

Moreover, the application of the response spectrum method to nonlinear analysis is not straightforward. Thus, in many cases, a nonlinear dynamic analysis is done, which requires an accelerogram representative of an earthquake expected at the site. Except for very few regions of the world where a set of recorded accelerograms are available, artificial earthquakes are used for the dynamic analysis. These earthquakes are defined by accelerograms that are consistent with a design spectrum. For performing this analysis in near-fault regions, this becomes even more significant. Because in near-fault most of the elastic energy arrives coherently in a single, intense, relatively long period pulse at the beginning of the record, representing the cumulative effect of almost all the seismic radiation from the fault [1]. An example of near-fault ground motion velocity is shown in Figure (1) where the velocity pulse can be seen clearly.

The available methodologies for obtaining spectrum compatible accelerograms based on the modification of historic records can be classified into three groups.

1. Those based on matching in the frequency domain by manipulation of the Fourier spectrum (e.g., Tsai [2])
2. Those grounded on wavelet adjustments to the recorded accelerograms at specific times (e.g., Lilhanand and Tseng [3]; Hancock et al [4])
3. Those centered on the manipulation of the wavelet coefficients obtained via continuous wavelet transform (e.g., Mukherjee and Gupta [5]).

This paper describes a wavelet-based ground motion simulation procedure. Wavelet analysis is well-suited to identify and preserve nonstationarity because of the multi scale nature of wavelet analysis, which facilitates the simultaneous evaluation of nonstationarity in the time and frequency domains. Wavelet analysis has been applied to engineering problems by several researchers. Gaupillaud et al [6] initiated the use of wavelet representation to analyze seismic data in oil exploration studies. Newland [7] used wavelets for analyzing vibration signals, Gurley and Kareem [8] examine a variety of applications for wavelet analysis including two general methods for simulating nonstationary processes and further developed this technique for engineering applications. The mother wavelet used in this article is based on Sua´rez, Montejo's work, a new wavelet based on the impulse response function of an underdamped oscillator.

2. Near-Fault Ground Motion

Near-fault ground motions are different from ordinary ground motions in that they often contain strong coherent dynamic long period pulses and permanent ground displace-ments. The dynamic motions are dominated by a large long period pulse of motion that occurs on the horizontal component per-pendicular to the strike of the fault, caused by rupture directivity effects. Near-fault

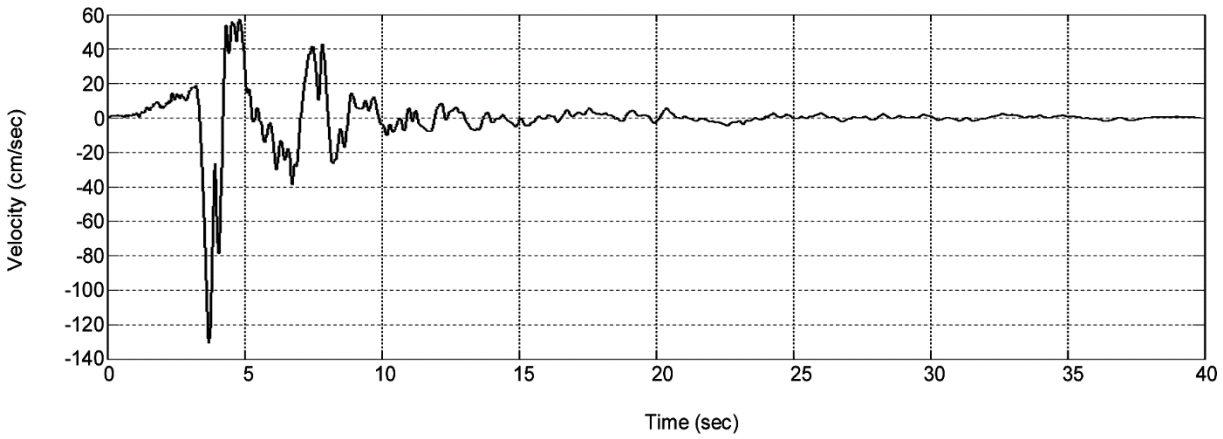

Figure 1. Example fault-normal, near-fault ground motion.

earthquakes are recognized as imposing extreme demands on structures [9]. Hence, it is very significant to understand the different requirements for seismic design of structures in near-fault regions. Near-fault effects become a focus of research after the Northridge (California, 1994), Kobe (Japan, 1995), Izmit (Turkey, 1999), and Chi-Chi (Taiwan, 1999) earthquakes. These earthquakes have caused extensive damage to the structure in the near-fault region. These ground motions will be referred to as "pulse-like ground motions". It is also noteworthy to take forward-directivity effects into account as it is one of the major causes of velocity pulses in the near-fault region. Forward rupture directivity effects occur when two conditions are met. The rupture front propagates toward the site, and the direction of slip on the fault is aligned with the site. This causes the waveform to arrive as single large pulse. The conditions for generating forward rupture directivity effects are readily met in strike-slip faulting, where the rupture propagates horizontally along strike either unilaterally or bilaterally, and the fault slip direction is oriented horizontally in the direction along the strike of the fault. However, not all near-fault locations experience forward rupture directivity effects in a given event. Backward directivity effects, which occur when the rupture propagates away from the site, give rise to the opposite effect, long duration motions having low amplitudes at long periods. Figure (2) schematically illustrates the partition of near-fault ground motions into the dynamic ground motion [10], which is dominated by the rupture directivity pulse, and the static ground displacement. For a strike-slip earthquake, the rupture directivity pulse is partitioned mainly on the strike-normal component, and the static ground displacement is partitioned on the strike-parallel component.

Near-fault recordings from recent earthquakes indicate that this pulse is a magnitude earthquakes may exceed those of larger earthquakes at intermediate periods (around 1 second). Several studies have proposed different types of features to of the narrow band pulse whose period increases

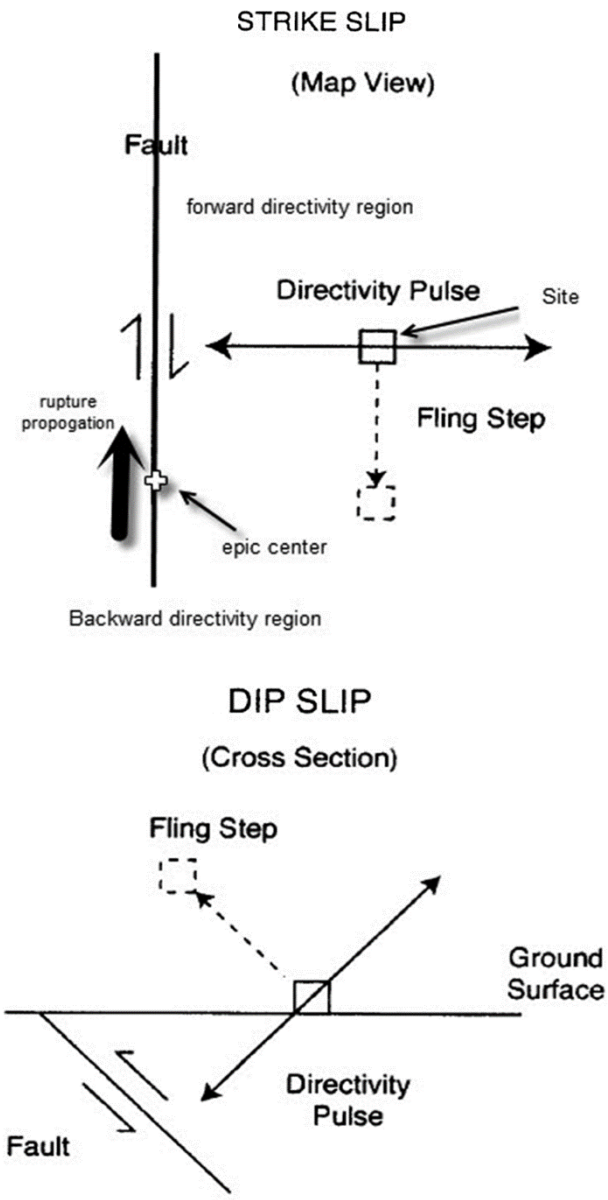

Figure 2. Schematic orientation of the rupture directivity pulse and fault displacement ('fling step') for strike-slip (left) and dip-slip (right) faulting.

with magnitude. This magnitude dependence pulse period causes the response spectrum to have a peak that its period increases with magnitude, such that the near-fault ground motions from moderate represent pulse-like near-fault effect [11]. To distinguish this kind of records from ordinary records, a quantitative method is needed. Before Baker's quantitative method, classification of near-fault motion was a personal judgment of a seismologist. These two parameters, large long-period pulse and fling step recorded within 25 km range, represent quality of records

not quantity. In this paper, Baker's method will be reviewed, then this method will be applied to find out whether the artificial generated records via wavelet transform can be classified as a near-fault motion or not. Baker [12] proposed a quantitative identification of near-fault ground motion using wavelet analysis. Summary of his study is described briefly in next section.

3. Baker's Method

For each ground motion under consideration, the largest velocity pulse was extracted using the wavelet decomposition and the coefficient with the largest absolute value is identified. The wavelet associated with this coefficient identifies the period and location of the pulse, as illustrated in Figure (3). (Note that a wavelet coefficient is equal to the energy of the associated wavelet, so the selected pulse is also the one with the largest energy).

Baker named this one as the main extracted pulse and the difference between the original and extracted pulse is residual. By using this procedure, a pulse can be extracted from any ground motion, whether a significant directivity pulse exists or not. For non-pulse-like records, however, the extracted pulse is typically a minor feature of the ground motion and the residual ground motion is nearly identical with the original motion.

The next step is to use these data and provide an indicator for pulse-like ground motion. Baker considered 402 records, all fault-normal ground motions in the Next Generation Attenuation (NGA) ground motion library (http://peer.berkeley.edu/nga) with magnitudes greater than 5.5 and recorded within 30 km of an event were selected and manually classified them as pulse-like (124 records), non-pulse-like (190 records) and ambiguous (84 records) records. He tries different ways to find a relation between original pulse and extracted pulses.

Finally, he found that two predicator variables, PGV ratio and energy ratio, can be a good representative of pulse indicator. Then, by means of logistic regression, he defined pulse indicator (PI) as follows:

$$PI = \frac{1}{1+e^{-23.3+14.6(PGVratio)+20.5(energyratio)}} \quad (1)$$

where *PGV* ratio is the peak ground velocity (PGV) of the residual record divided by the original record's PGV, and energy ratio is the energy of the residual record divided by the original record's energy (where energy can be computed as the cumulative squared velocity of the signal or equivalently, as the sum of the squared discrete wavelet coefficients. Pulse indicator takes values between 0 and 1, with high values providing a strong indication that the ground motion is pulse- like records with scores above 0.85 and below 0.15 are classified as pulses and non-pulses,

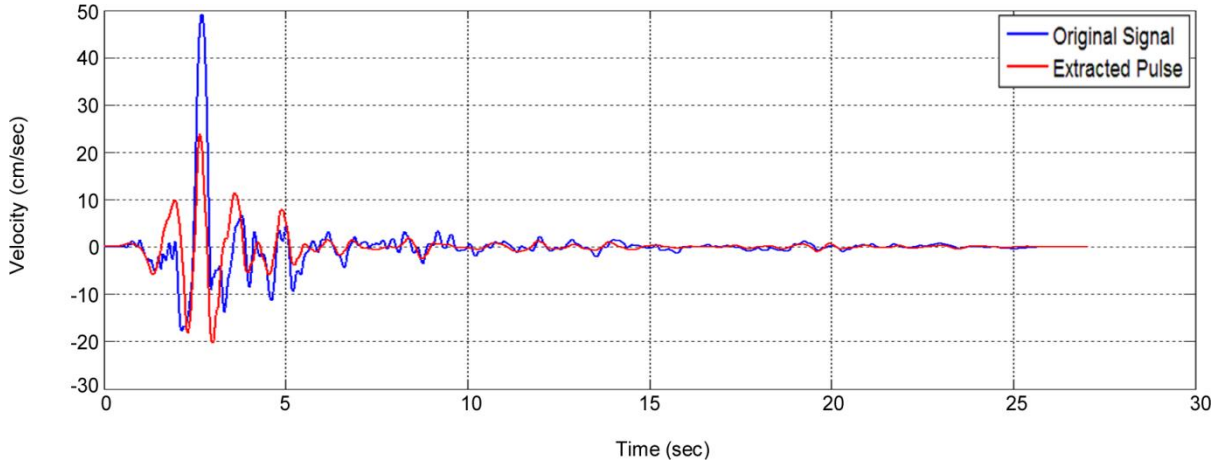

Figure 3. Illustration of the decomposition procedure used to extract the pulse portion of a ground motion (the fault-normal component of the 1984 Coyote Lake).

respectively, and records with pulse indicator between 0.85 and 0.15 classified as ambiguous. Desired near-fault ground motions have pulses arriving early in their velocity time history. He proposed using cumulative squared velocity (CSV) of original and extracted pulses in which 10% of total CSV of extracted pulse ($t_{10\%pulse}$) should reach before 20% of total CSV of original signal ($t_{20\%original}$) as shown in Figure (4). Otherwise, signal should be excluded.

And the final criteria is, since the motion may be very simple for far-field records, it is possible to have a velocity time history as a pulse where soil inelastic properties will filter motions. To exclude these far-field pulse-like motion, Baker proposed to put a limit of PGV>30cm/s on records. It should be noted that a given record should satisfy all three potential criteria simultaneously.

1. The pulse indicator value, as defined in Equation (1), is greater than 0.85.
2. The pulse arrives early in the time history, as indicated by t20%,orig values that are greater than t10%, pulse
3. The original ground motion has a PGV of greater than 30 cm/sec.

These three criteria identify ground motions of engineering interest because of their large amplitude and potential directivity effects. The three criteria described earlier will be used to identify whether the generated artificial records have pulse or not.

4. Wavelet Transform

Earthquake motions are, by their very nature, transient and non-stationary process. A recently developed wavelet analysis has emerged as a powerful tool to analyze a transient signal providing information simultaneously both in time and frequency domains. In wavelet representation, the basic functions are localized and contained in finite time domains. Gaupillaud [6] initiated the use of wavelet representation to analyze seismic data in oil exploration studies. Subsequently, other researchers have contributed to the development of the methodology of wavelet analysis. Newland [7], used wavelets for analyzing vibration signals, and further developed this technique for engineering applications. Recently, few applications of wavelet analysis have been made to geotechnical earthquake engineering problems. Some of the researchers (Iyama and Kuwamura, [13]; Refooei et al [14]; Ghodrati Amiri et al [15]) developed the wavelet analysis for generating earthquake records. The aim of this paper is to generate artificial near-field earthquake records compatible with predicted spectra by the wavelet transform. Wavelet transform theory is appeared as a powerful tool for time-frequency analysis to accurately model the non-stationary processes in term of statistical functional of their wavelet coefficients. The wavelet transform is similar to the Fourier transform as it breaks a signal

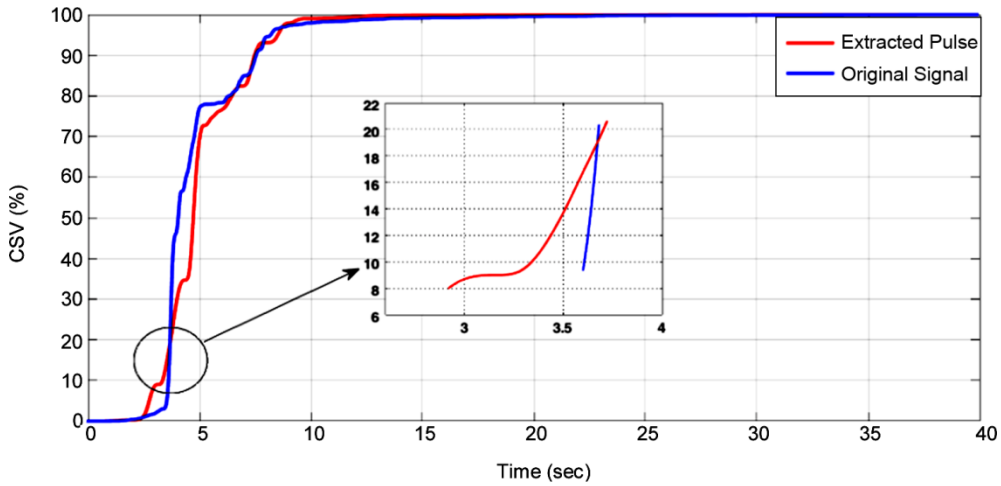

Figure 4. An early-arriving pulse (1994 Northridge). Cumulative squared velocities. The times corresponding to $t_{20\%,orig}$ and $t_{10\%pulse}$ are marked with vertical lines.

down into its constituents, whereas the FT breaks the signal into a series of sine waves of different frequencies, the WT breaks the signal into its wavelets, which are scaled and shifted versions of the so-called mother wavelet. In general, the WT of the signal, *x(t)*, is defined as a following inner product:

$$C(s,p)=\int_{-\infty}^{+\infty} f(t)\psi_{s,p}(t) \tag{2}$$

where $\psi_{s,p}(t)$ is the mother wavelet function and is defined as:

$$\psi_{s,p}(t)=\frac{1}{\sqrt{s}}\psi(\frac{t-p}{s}) \tag{3}$$

The family of continuously translated and dilated wavelets is generated from mother wavelet ψ, where p is the translation parameter, corresponding to the position of the wavelet as it is shifted through the signal, s is the scale dilation parameter determining the width of the wavelet. The wavelet coefficients, $C(s,p)$, represent the correlation (in terms of the time-scale functions) between the wavelet and a localized section of the signal. In other words, the CWT coefficients can be considered as a correlation coefficient and a measure of analogy between the wavelet and the signal in the time-scale plane. The higher the coefficient is, the more the similarity will be. If the signal has a major component of the frequency corresponding to the given scale, then the wavelet at this scale is close to the signal at the particular location and the corresponding wavelet transform coefficient, determined at this point, has a relatively large value. In all practical applications, the coefficients *C*(*s*,*p*) are modified somehow to achieve a given objective before they are transformed back to the original time domain. The signal $f(t)$ can be retrieved with the so-called reconstruction formula:

$$f(t)=\frac{1}{K_\psi}\int_{s=0}^{\infty}\int_{-\infty}^{\infty} C(s,p)\psi_{(s,p)}(t)\,dp\,\frac{ds}{s^2} \tag{4}$$

The constant Kw depends on the mother wavelet selected, and is defined as:

$$K_\psi=\int_0^{\infty}\frac{|\psi(\omega)|^2}{\omega}d\omega<\infty \tag{5}$$

The mother wavelet used in this article is based on Sua´rez, Montejo's work [16]. It is impulse response function of an under damped oscillator. The mother wavelet has the following form:

$$\psi(t)=e^{-\zeta\Omega|t|}sin\Omega t \tag{6}$$

where ζ and Ω are two parameters that govern the decrement and the time variation of the wavelet. They can be identified with the damping ratio and natural frequency of a single degree of freedom oscillator. Figure (5) shows the propose wavelet for the values of the parameters ζ = 0.05 and Ω = π.

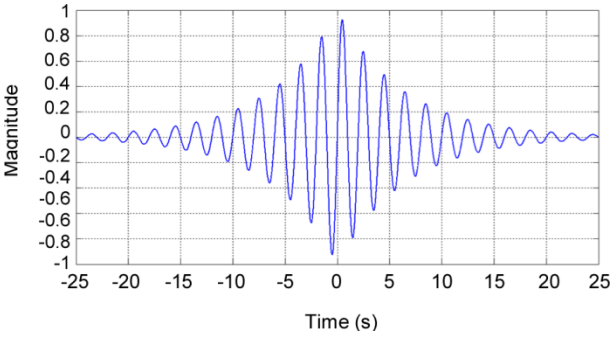

Figure 5. The proposed Impulse Response Wavelet for ζ = 0.05 and $\Omega = \pi$.

As Sua´rez and Montejo explain, the time function f(t) is the ground acceleration $\ddot{X}_g(t)$ due to an earthquake. It is convenient to re-write Eq. (4) as follows:

$$\begin{aligned}\ddot{X}_g(t)&=\int_{s=0}^{\infty}\left(\int_{p=-\infty}^{\infty}\frac{1}{s^2}C(s,p)\psi_{(s,p)}(t)\,dp\right)ds\\&=\int_0^{\infty}D(s,t)\,ds\end{aligned} \tag{7}$$

The constant $K\Psi$ was set equal to 1 because here we are not interested in retrieving the original time function. In other words, the function $\ddot{X}_g(t)$ will be the accelerogram of the modified earthquake motion, and from here we refer $D(s,t)$ as detail function. In practice, a set of n discrete values s_j of

the continuous scale *s* are used.

$$s_j = 2^{\frac{j}{8}} \quad j = -(n_0 - 1), -(n_0 - 2), \ldots . -(n_0 - n) \qquad (8)$$

where *n* is the number of discrete values of s_j and n_0 is a selected integer. In practical applications, the ground acceleration signal $\ddot{X}_g(t)$ is always sampled at equal time intervals Δt. We will assume that the accelerogram is sampled at N discrete times t_k. Since p is a time scale as well, it will also be discretized as a set of N values. The discrete coefficients of the wavelet transform given by Eq. (2) will be calculated using the approximate Expression.

$$C(s_j, p_i) \cong \frac{\Delta t}{\sqrt{s_j}} \sum_{k=1}^{N} f(t_k) \psi\left(\frac{t_k - p_i}{s_j}\right) \qquad (9)$$
$$j = 1, \ldots, n \qquad i = 1, \ldots N$$

In terms of the discrete scales, the detail functions are then defined:

$$D(s_j, t_k) \cong \frac{\Delta p}{s_j^{5/2}} \sum_{k=1}^{N} C(s_j, p_i) \psi\left(\frac{t_k - p_i}{s_j}\right) \qquad (10)$$
$$j = 1, \ldots, n \qquad i = 1, \ldots, N$$

The detail function have the predominant frequency that can be defined by examining the dilated wavelet obtained from Eq. (6).

$$\psi\left(\frac{t-p}{s_j}\right) = e^{-\zeta\Omega\left|\frac{t-p}{s_j}\right|} \sin\left(\frac{\Omega t - p}{s_j}\right) \qquad (11)$$

The predominant frequency ω_j and period T_j of each detail function are:

$$\omega_j = \frac{\Omega}{s_j}; \quad T_j = \frac{2\pi}{\Omega} s_j \qquad (12)$$

Based on Sua´rez and Montjo's work for the numerical implementation, the values of n_0=51 and n=63 are used herein. With these values, the index j goes from 50 to 12, and the scale s_j takes values from 0.0131 to 2.8284. According to Eq. (12), the frequencies ω range from 1.1107 rad/s (T = 5.657 s) to 238.904 rad/s (T = 0.0263 s). Table (1) shows the values of the scale s_j, the predominant frequency in rad/s and Hertz, and the period for a few detail functions. Figures (6) and (7) indicate few detail functions and the corresponding Fourier Transform.

Table 1. The scale, dominant frequency and period of selected detail functions.

Detail#	j	Sj	ω_j(rad/s)	Tj(s)	f(Hz)
1	-50	0.0131	239.1	0.0263	38.05
10	-41	0.0287	109.6	0.0573	8.33
20	-31	0.0682	46.1	0.1363	7.34

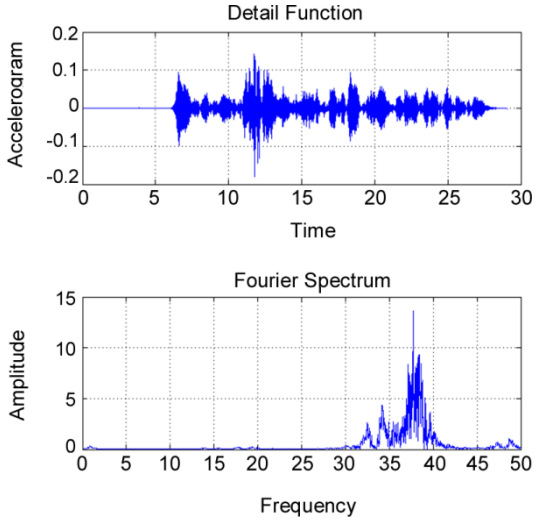

Figure 6. Detail function #1 (j = 50) and the magnitude of its Fourier transform with a dominant frequency at 38 Hz.

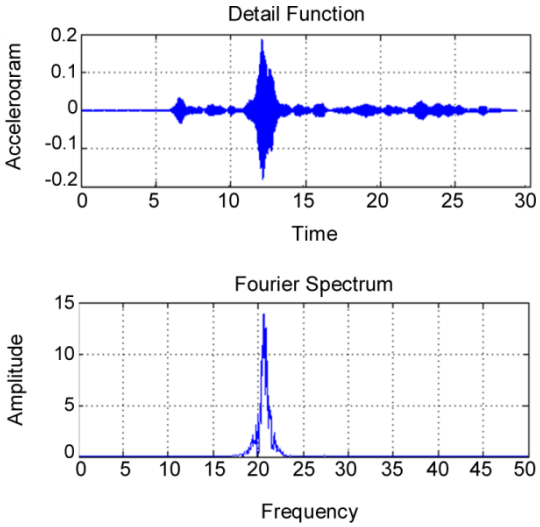

Figure 7. Detail function #7 (j = 44) and the magnitude of its Fourier transform with a dominant frequency at 22 Hz.

The ground response spectrum of original accelerogram is first calculated at the values of the periods T_j defined by the discrete values of s_j in Eq. (12). Then the ratios γ_j between the values of the target and the calculated spectra are computed. Then, the detail functions $D(s_j, t_k)$, are multiplied by these ratios and a new accelerogram is

calculated using Eq. (7). The response spectrum of this updated accelerogram is calculated, a set of new ratios γ_j are computed and the previous detail functions are corrected. The process continues until all the ratios γ_j become sufficiently close to 1.

$$\gamma j = \frac{\left[S_a(T_j)\right]_{target}}{\left[S_a(T_j)\right]_{reconstructed}} \quad (13)$$

5. Generating Ground Motion

It is desired to modify selected records so they will be compatible with the near-fault ground design spectrum prescribed in the standard No. 2800 of the Iranian National Building Code (INBC) for seismic zone 1 (seismically active zone) and soil type 2 (rock) [17]. The target spectrum is shown in Figure (8).

Figure 8. The INBC-zone 1-soil II design spectrum.

To illustrate the procedure introduced here, two sets of five records are considered to represent ordinary and near-fault motions. These records were selected from NGA database [18]. Table (2) and (4) summarize the principle properties of ordinary and near-fault records respectively.

Table 2. Characteristic of ordinary ground motion.

NGA Number	Event	Year	Station	Mag	R_{rup}(Km)	V30 (m/s)	Mechanism	PGA(g)	PGV(cm/s)
28	Parkfield	1966	Cholame - Shandon Array #12	6.19	17.6	408.9	Strike-Slip	0.06	5.81
33	Parkfield	1966	Temblor pre-1969	6.19	16	527.9	Strike-Slip	0.35	21.47
40	Borrego Mtn	1968	San Onofre - So. Cal. Edison	6.63	129.1	442.9	Strike-Slip	0.041	3.67
57	San Fernando	1971	Castaic - Old Ridge Route	6.61	22.6	450.3	Reverse	0.32	15.64
58	San Fernando	1971	Cedar Springs Pump House	6.61	92.6	477.2	Reverse	0.024	2.87

Table 3. Baker's parameters for ordinary records before and after matching.

NGA Number	Event	Before Matching Process			After Matching Process		
		PGV	PI	Late	PGV(cm/s)	PI	Late
28	Parkfield	5.81	0.0036	0	56	0.98	1
33	Parkfield	21.64	0.35	1	58	0.0109	1
40	Borrego Mtn	3.6	0.0005	1	57	0.09	1
57	San Fernando	15.7	0.00066	1	57	0.0017	1
58	San Fernando	2.87	0.075	1	71	0.0034	1

Table 4. Characteristic of pulse-like ground motion.

NGA Number	Event	Year	Station	Mag	R_{rup} (Km)	V30 (m/s)	Mechanism	PGA (g)	PGV (cm/s)
723	Superstition Hills-02	1987	Parachute Test Site	6.54	0.9	370	Strike-Slip	0.45	112
645	Whittier Narrows-01	1987	LB - Orange Ave	6	24.5	350	Reverse-Oblique	0.25	32
779	Loma Prieta	1989	LGPC	6.93	5.4	477.7	Reverse-Oblique	0.96	108.68
983	Northridge-01	1994	Jensen Filter Plant Generator	6.69	5.9	525.8	Reverse	0.57	76
1086	Northridge-01	1994	Sylmar - Olive View Med FF	6.69	5.3	440.5	Reverse	0.84	130

Wavelet transform is used to modify ordinary records and match their spectra with the target spectra. For Parkfield earthquake (Cholame - Shandon) the original and final velocity history which is compatible with the INBC spectrum is shown in Figure (9). It is clear that the velocity history of the original record does not have any significant pulse. This is important to keep in mind that when we are talking about single large pulse caused by directivity, it is inherently a velocity pulse. Figure (10) shows the spectrum matching procedure applied to San Fernando record. Table (3) provides information about the three criteria, recommended by Newland [7], before and after matching process.

Column "Late" indicates the second criteria, it shows whether the pulse identified by baker's

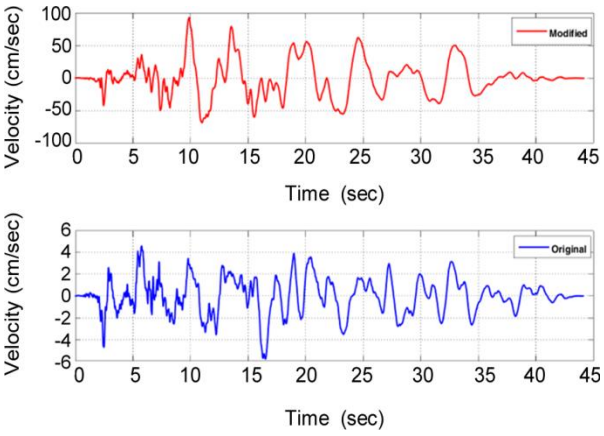

Figure 9. Top: velocity history of the Modified record for Parkfield (Sholame - Shandon) earthquake. Bottom: Original velocity history.

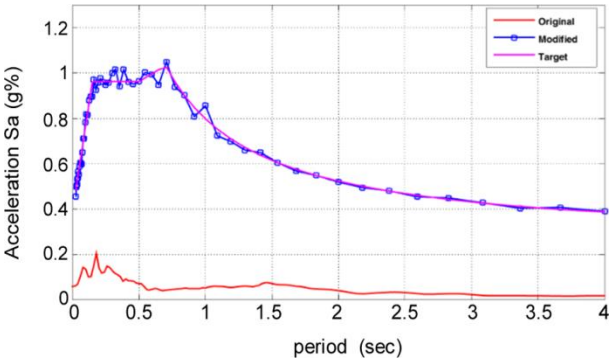

Figure 10. The target spectrum and the spectra of the original and modified Parkfield record.

method arrive early in time history or not. By looking at the right-hand column of the table, it is clear that all the ordinary records satisfied the third criteria (PGV > 30cm/sec) after spectrum matching process. In just one case after matching process, wavelet analysis can identify a pulse with PI greater than 0.85 but it does not satisfy the second criteria, which states that the pulse should arrive early in velocity time history.

Now let's consider the second set with pulse-like ground motions. It can be clearly seen from the velocity time history that all of these records contain distinct velocity pulses. Table (5) shows the three criteria for pulse-like records before and after matching process.

For Superstition earthquake, the original and modified velocity history of the record is shown in Figure (11). Figure (12) shows the spectrum matching process.

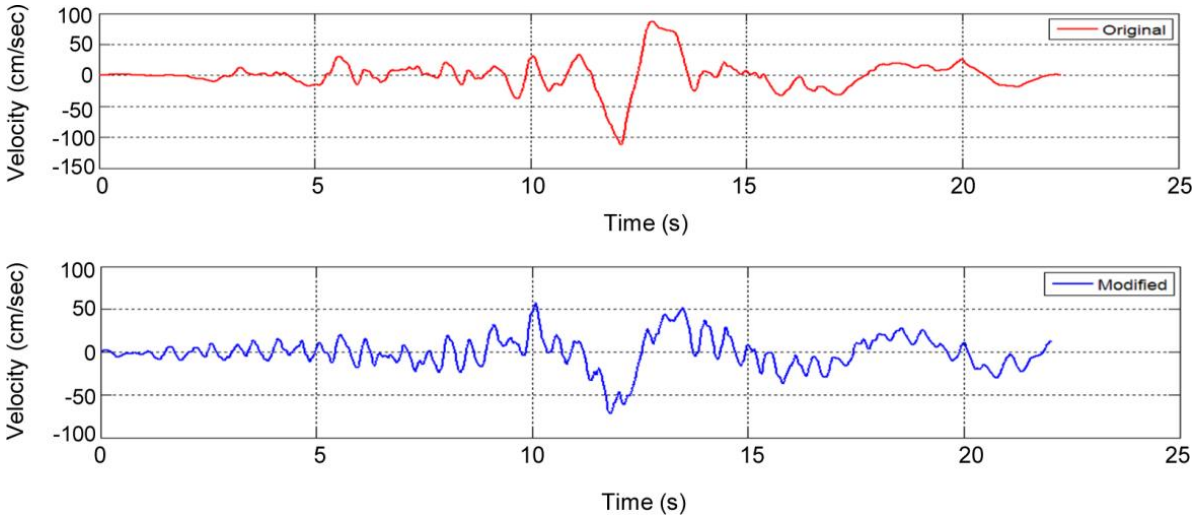

Figure 11. Top: velocity history of the original record for Superstition earthquake. Bottom: modified velocity history.

Table 5. Baker's parameters for pulse-like records before and after matching.

NGA Number	Event	Before Matching Process			After Matching Process		
		PGV	PI	Late	PGV(cm/s)	PI	Late
723	Superstition Hills-02	112	0.999	0	68	0.98	0
645	Whittier Narrows-01	32	0.999	0	79.3	0.87	0
779	Loma Prieta	108.68	0.89	0	57.28	0.96	0
983	Northridge-01	76	0.99	0	62	0.92	0
1086	Northridge-01	130	0.99	0	68	0.87	0

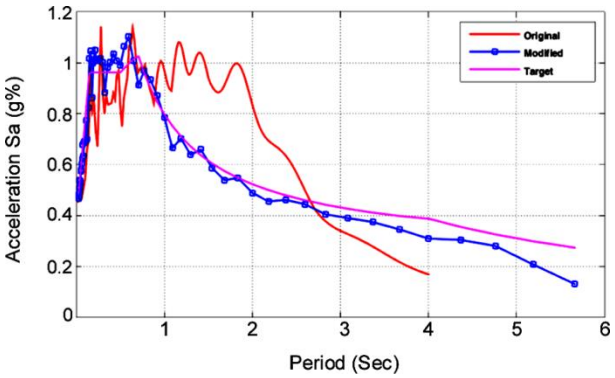

Figure 12. The target spectrum and the spectra of the original and modified Superstition record**.**

6. Conclusion

When dynamic time history analyses are to be performed, the seismic input needs to be defined as a time history of accelerations. To comply with code requirements, the spectral acceleration series used, must be compatible with the design spectrum.

Wavelet transform is proven as a powerful tool for obtaining a set of spectrum-compliant time histories, so Wavelet transform is applied to generate sets of near-fault accelerogram compatible with INBC near-fault code herein. First these synthetic records are generated from ordinary motions. After matching process, these records have been investigated by Baker's method to detect a velocity pulse in their time history, however; no velocity pulse has been found. In other words, these records would not satisfy the three criteria introduced by Baker's method, and despite of their match spectra, they cannot be classified as near-fault ground motions. As a consequence, if a dynamic time history analysis was performed based on this synthetic records, the result would not be suitable for a near fault region since these records don't have the most important feature of the near fault region which is a long period pulse.

On the other hand, it seems that applying this procedure to a pulse-like record, they will reserve its pulse caused by forward directivity besides spectra matching. Therefore, the result of a dynamic time history analysis can be more realistic since these records have the long period pulse as well as their matched spectra.

References

1. Ebrahimian, B. and Graves, R. (2008) Simulation of near field strong ground motions at Tombak site in Iran using hybrid method. *The 14th World Conference on Earthquake Engineering*, October 12-17, 2008, Beijing, China.

2. Tsai, N.C. (1972) Spectrum-Compatible Motions for Design Purposes. *J. Eng. Mech. Div.*, ASCE, **98**, 345-356.

3. Lilhanand, K. and Tseng, W.S. (1988) Development and application of realistic earthquake time histories compatible with multiple damping design spectra. *Proceedings of the 9th WCEE*, **2**, Tokyo-Kyoto, Japan, 819-824.

4. Hancock, J., Watson-Lamprey, J., Abrahamson, N.A., Bommer, J.J., Markatis, A., McCoy, E., and Mendis, R. (2006) An improved method of matching response spectra of recorded earthquake ground motion using wavelets. *J. Earthq. Eng.*, **10** (Special Issue 1), 67-89.

5. Mukherjee, S. and Gupta, V.K. (2002) Wavelet-Based generation of spectrum compatible time-histories. *Soil Dyn. Earthq. Eng.*, **22**(9-12), 799-804.

6. Gaupillaud, P., Grossmann, A., and Morlet, J.

(1984) Cycle-octave and related transforms in seismic signal analysis. *Geoexploration*, **23**, 85-102.

7. Newland, D.E. (1993) *An Introduction to Random Vibrations, Spectral and Wavelet Analysis*. UK: Longman.
8. Gurley, K. and Kareem, A. (1999) Applications of wavelet transforms in earthquake wind and ocean engineering. *Engineering Structures*, **21**, 149-167.
9. Krawinkler, H., Alavi, B., and Zareian, F. (2005) 'Impact of Near-Fault Pulses on Engineering Design.' In: *Directions in Strong Motion Instrumentation*, Springer Netherlands, 83-106.
10. Somerville, P.G. (2002) Characterizing near fault ground motion for the design and evaluation of bridges. *Proceedings of the Third National Seismic Conference and Workshop on Bridges and Highways.*
11. Bray, J.D. and Rodriguez-Marek, A. (2004) Characterization of forward-directivity ground motions in the near-fault region. *Soil Dynamics and Earthquake Engineering*, **24**(11), 815–828.
12. Baker, J. (2007) Quantitative classification of near-field ground motion using wavelet analysis. *Bulletin of the Seismological Society of America*, **97**(5), 1486–1501.
13. Iyama, J. and Kuwamura, H. (1999) Application of wavelet to analysis and simulation of earthquake motions. *Earthquake Engineering and Structure Dynamics*, **28**(3), 255-272.
14. Refooei, F.R., Mobarake, A., and Ahmadi, G. (2001) Generation of Artificial Earthquake Records with a Nonstationary Kanai-Tajimi Model. *Engineering Structures*, **23**(7), 827–37.
15. Ghodrati Amiri, G., Ashtrai, P., and Rahami, H. (2006) New development of artificial record generation by wavelet theory. *Structural Engineering and Mechanics*, **22**(2), 185-195.
16. Suarez, L.E. and Montejo, L.A. (2005) Generation of artificial earthquakes via the wavelet transform. *Int. J. Solids Struct.*, **42**, 5905–5919.
17. Building and Housing Research Center of Iran (2012) *Iranian Code of Practice for Seismic Resistant Design of Buildings, Standard No. 2800*. 4th Ed.
18. PEER Strong Motion Database: http://peer.berkeley.edu/nga.